






## Research Article

# Physicochemical Characterization of Star Anise Silver Nanoparticles Incorporated Chitosan Biomaterial for Absorb Water and Cure Wounds

M. Prabhakar <sup>1</sup>, Gomathi Kannayiram <sup>2</sup>, S. Prakash <sup>1</sup>, M. Saravanakumar,<sup>1</sup>  
Sangeetha Krishnamoorthi,<sup>1</sup> S. Sendilvelan <sup>3</sup>, P. Rahul Senthana,<sup>1</sup> T. S. Ashikmon,<sup>1</sup>  
M. Karthik,<sup>1</sup> and Haiter Lenin <sup>4</sup>

<sup>1</sup>Department of Mechanical Engineering, Aarupadai Veedu Institute of Technology, Vinayaka Mission Research Foundation, Tamilnadu 603104, India

<sup>2</sup>Department of Biotechnology, Dr. M.G.R. Educational and Research Institute, Chennai 600095, Tamilnadu, India

<sup>3</sup>Department of Mechanical Engineering, Dr. M.G.R. Educational and Research Institute, Chennai 600095, Tamilnadu, India

<sup>4</sup>Department of Mechanical Engineering, WOLLO University, Kombolcha Institute of Technology, Kombolcha, Post Box no.: 208, Ethiopia

Correspondence should be addressed to Haiter Lenin; [haiter@kiot.edu.et](mailto:haiter@kiot.edu.et)

Received 15 May 2022; Accepted 31 May 2022; Published 4 July 2022

Academic Editor: Ibrahim H. Alsohaimi

Copyright © 2022 M. Prabhakar et al. This is an open access article distributed under the Creative Commons Attribution License, which permits unrestricted use, distribution, and reproduction in any medium, provided the original work is properly cited.

Chronic wounds threaten the geriatric society worldwide irrespective of their social status. The current treatment approach to cure chronic ailments is associated with its demerits. A novel treatment approach that is coordinated is required to adsorb water from wounds and cure chronic wounds. Star anise condiment used in the Indian kitchen is shown to have the potency to cure various ailments. In this study, silver nanoparticles were prepared using the star anise extract. The biological potency of star anise extract was confirmed through Gas Chromatography Mass Spectroscopy, antioxidant assay, and anti-inflammatory study. From the DPPH assay result, it was inferred that star anise extract was able to scavenge the free radicals at the concentration of 10  $\mu\text{g}/\text{ml}$  using the aqueous extract silver nanoparticles were prepared. The prepared particles were characterized by UV-visible, scanning electron microscopy, and their biological efficacy was determined for their potency against bacteria and prevention of protein aggregation. The anti-inflammatory assay suggests that nanoparticles prevent the aggregation of proteins in a dose-dependent manner. IC<sub>50</sub> was found to be 20  $\mu\text{g}/\text{ml}$ . The synthesized nanoparticle was incorporated into the chitosan biomaterial and characterized by various physicochemical parameters such as differential scanning calorimetry, scanning electron microscopy, FTIR, and thermogravimetric analysis. According to the findings, silver nanoparticles incorporated in chitosan biomaterials can be used to adsorb water from wounds and wound healing materials.

## 1. Introduction

The concept of nanotechnology is trending worldwide in various fields [1]. Nanotechnology is a unique field with a blend of various interdisciplinary fields [2, 3]. Chronic wound healing is a very difficult process due to the imbalance of various molecular events [4]. Due to this healing of chronic wounds gets delayed. When healing gets delayed, it leads to an infectious wound due to bacterial contamination [5].

The normal wound dressing may not be useful for chronic wounds as it cannot promote healing, gaseous exchange, and angiogenesis [6]. Traditionally, silver-based ointments are used for the healing process as they are antimicrobial [7]. Delay in the healing of chronic wounds is the multifactorial factors like improper inflammation and bacterial contamination; on this basis, antimicrobial creams or agents do not solve the purpose [8].

Green-synthesized silver nanoparticles (AgNP) using herbal plants and their products are shown to be much more

potent when compared to the normal silver-based ointments [9]. The potency of the AgNP was enhanced due to the synergistic effect of plant extract involved in the process of AgNP formation [9].

Star anise (*Illicium verum*) plays an important role in Indian kitchen spices. The star anise was found to cure various health ailments [10]. Star anise is the source of shikimic acid which is an important ingredient in the preparation of anti-flu (Tamiflu) drug which prevents the severity of the influenza virus [11]. Earlier research work claims that its potent active components make the star anise have high antioxidant potency and also prevent a low-grade inflammatory response [10, 11]. The bioactive components in the star anise act as reducing agents in the formation of silver NP. The potency of the star anise and silver together as an AgNP might increase the wound healing by preventing the growth of bacteria, scavenging the free radicals in the wound environment, and also might prevent an unwanted inflammatory response.

As chronic wounds mostly affect geriatric patients, repeated application of the drug in the wound area would be difficult for them [12]. Moreover, to obtain proper healing, there should sustain drug release approach irrespective of the microenvironment of the wound [13]. To release the drug in sustained manner, incorporation into a polymer would be the choice. Also, if the polymer acts as a temporary, it would be even better to achieve the proper healing [14]. A lot of polymers are under research, and few have been used for patients. Among such polymers, chitosan has shown to be much promising as it has a poor immunologic response, allows gaseous exchange, has good tensile strength, has higher mechanical strength with good biocompatibility, and provides moisture, and it is also capable of delivering the drug in a sustained manner [15, 16].

The objective of the study is to make a potent biomaterial for dermal wound healing. To achieve in this, we study star anise AgNP (SA-Ag-NP) was synthesized and incorporated into chitosan biomaterial. The synthesized Ag-NP was characterized by scanning electron microscopy. The incorporated biomaterial was characterized by scanning electron microscopy, FTIR, dynamic scanning calorimetry, and thermogravimetric analysis.

## 2. Materials and Methods

All the chemicals used in this study were purchased from SD chemicals India. The chemicals purchased were of analytical grade.

### 2.1. Methods

**2.1.1. Preparation of Star Anise Ethanol and Aqueous Extract.** About 250 g of star anise was purchased from Sidha medical store and powdered. The powdered star anise was soaked in ethanol at a ratio of 1 : 3. The soaked star anise was filtered after three days. The filtrate was concentrated by evaporating the solvent using a rota evaporator. The extract obtained was used for gas chromatography-mass spectros-

copy analysis (GCMS) and antioxidant study. For aqueous extract, 100 g of powdered star anise was added to the 500 ml of boiling water. The aqueous solution was boiled for 20 minutes. After 20 minutes, it was cooled completely and filtered. The filtered solution was stored and was used for the preparation of AgNP [16].

**2.1.2. GCMS Analysis.** GCMS technique was used in this study to identify the phytochemicals present in the extract. GCMS analysis of the ethanol extract of star anise was performed using the GC Shimadzu Qp 2020 system software adopted to handle mass spectra [17].

**2.1.3. DPPH Assay.** The antioxidant potency of the extract was determined by a DPPH scavenging assay. DPPH is commercially available as a free radical. Briefly, 0.1 mM solution of DPPH was prepared using ethanol. From the prepared solution, 0.9 ml of DPPH solution was added to the micro-fuge tube; to this, varied concentration of the extract was added in the range 5, 10, 15, 20, 25, and 50  $\mu\text{g/ml}$ . The tubes were incubated for 30 minutes, and the absorbance was measured at 517 nm [18].

**2.1.4. Hydroxyl Radical Scavenging Assay.** The hydroxyl radical scavenging assay was done by following the protocol mentioned by Halliwell and Gutteridge. As described in the reference, Fenton's reagent was produced to generate hydroxyl radicals. The basis of this assay is to measure the degradation formed from 2-deoxy-D-ribose. Briefly, the known amount of Fenton reagent varied concentration plant extract was added. To this, 2-deoxy-D-ribose was also added. After 1 hr of this reaction mixture cold, TBA was added followed by HCL. The mixture was heated and cooled, and it was estimated at 532 nm. Extract concentrations used for the assay were in the range of 5, 10, 15, 20, 25, and 50  $\mu\text{g/ml}$  [19].

**2.1.5. Preparation of Star Anise Silver Nanoparticle (SA-Ag-NP).** The concentration of silver nitrate used was 1 mM. Briefly, 180 ml of silver nitrate solution (1 mM) was mixed with 20 ml of star anise aqueous extract, and the solution was stirred in the dark chamber. The formation of SA-Ag-NP was observed by the color change from a pale color to dark brown color.

**2.1.6. Characterization of SA-Ag-NP by UV-Visible Spectrophotometer.** The formation of SA-Ag-NP was observed in UV-visible spectrophotometer (Shimadzu). The spectrum was taken in the range of 200–800 nm [20].

**2.1.7. Scanning Electron Microscopy.** The surface morphology and size of the AgNP were measured by SEM analysis. According to the protocol given in the reference, the sample was prepared and analyzed using (Zeiss EVO 40) scanning electron microscope [21].

**2.1.8. Antimicrobial Assay.** The antimicrobial activity of the SA-Ag-NP was tested through the agar well diffusion method. In this, *Bacillus subtilis* was used as model organisms to get the results for minimum inhibitory concentration. Briefly, the agar plate was uniformly spread with

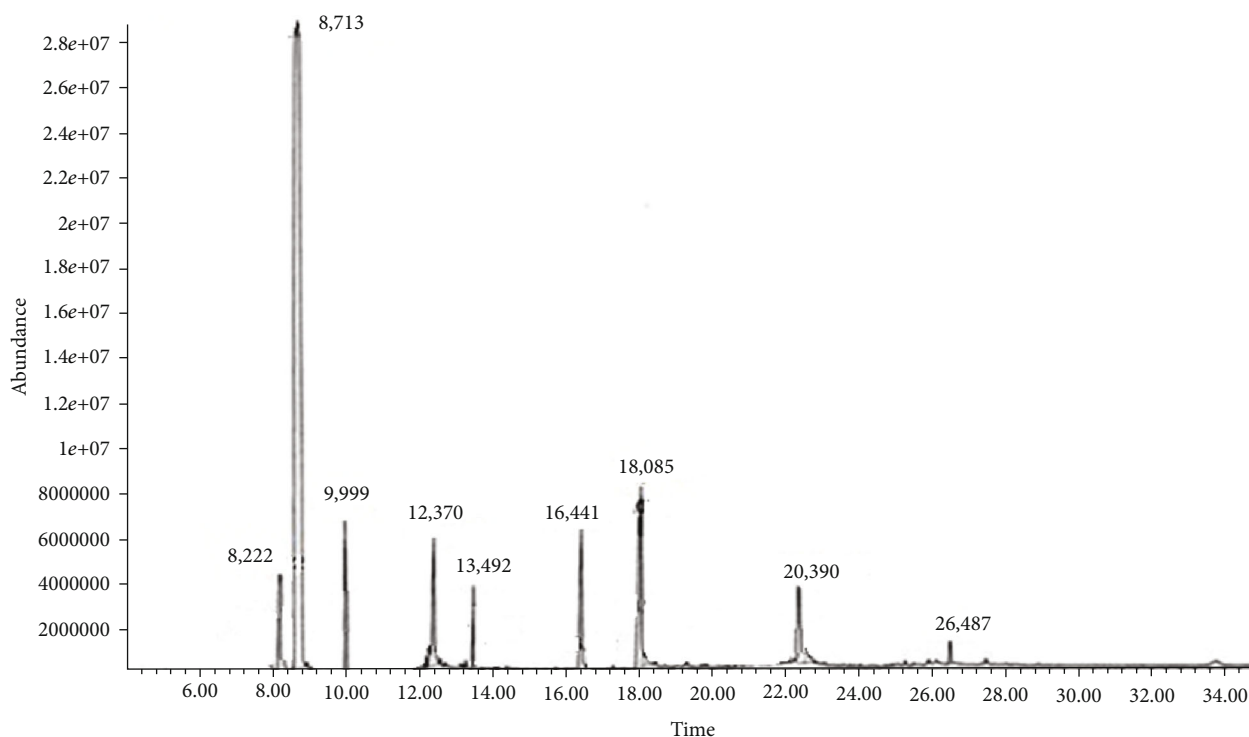


FIGURE 1: GCMS analysis of star anise extract.

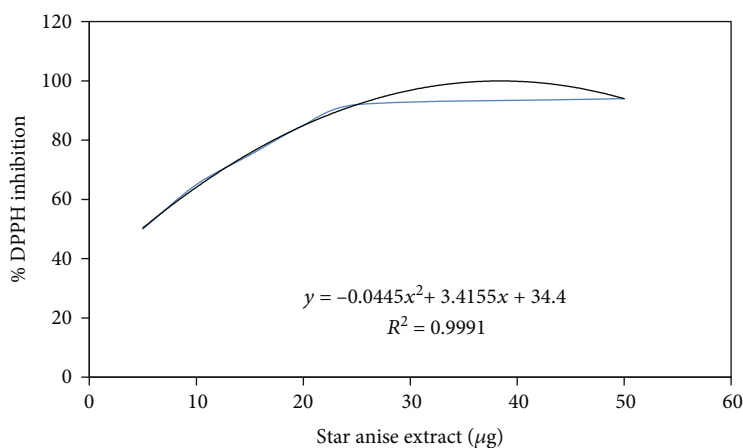


FIGURE 2: Inhibition of DPPH radical by star anise extract.

bacterial culture. The agar plate well was cut, and varied concentrations of nanoparticles were added to the well. The plates were incubated overnight at 37°C, and the zone of inhibition was measured [4].

**2.1.9. Protein Aggregation or Denaturation Assay.** A protein aggregation or denaturation assay was done to prove the potency of SA-Ag-NP as an anti-inflammatory agent. A briefly varied concentration of the extract was added to the bovine serum albumin and heated. The reaction was cooled. The ability of SA-Ag-NP to the prevention of aggregation of protein was studied at 600 nm. The less scattering suggests that SA-Ag-NP effectively prevents the aggregation of proteins.

**2.1.10. Preparation SA-Ag-Np Chitosan Biomaterial.** 0.5% chitosan was mixed with acetic acid; to this, AgNP was added and stirred for 10 minutes at 40°C; after ten minutes, glutaraldehyde solution was added as a cross-linking agent and continued for stirring for another ten minutes. After that, solution was poured on the Teflon tray and dried inside the laminar hood. The dried biomaterial sheet was analyzed for physicochemical characterization.

**2.1.11. FTIR Analysis.** FTIR analysis was carried out to check whether nanoparticles were infused into the chitosan biomaterial. The Ag-NP-incorporated chitosan biomaterial was characterized using FTIR (Perkin Elmer). All spectra were recorded in the range 300-4000  $\text{cm}^{-1}$  [22].

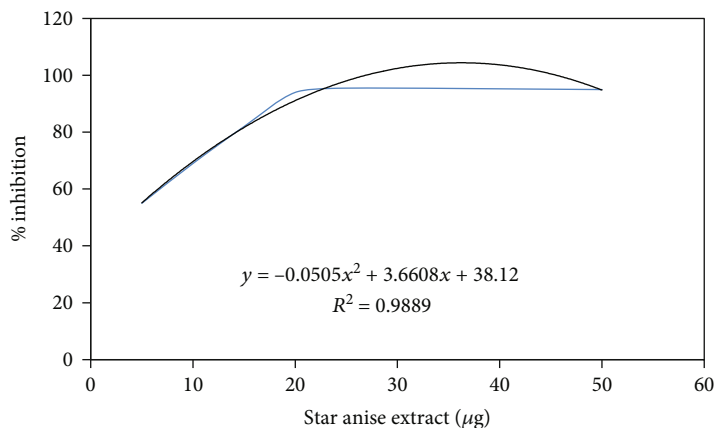


FIGURE 3: Inhibition of hydroxyl radical by star anise extract.

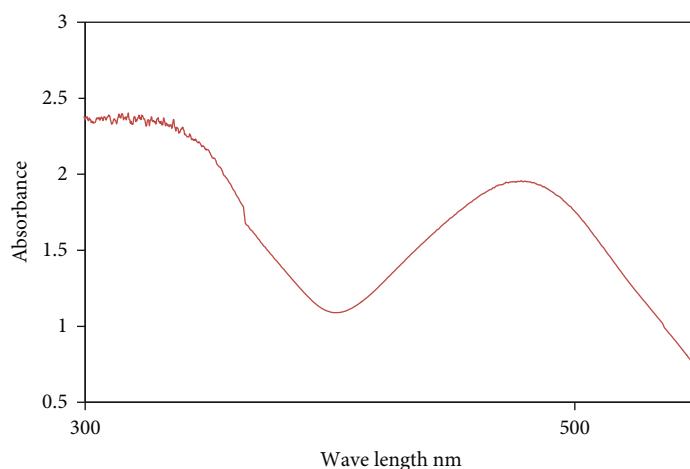


FIGURE 4: UV-Vis spectrum of SA-Ag-NP.

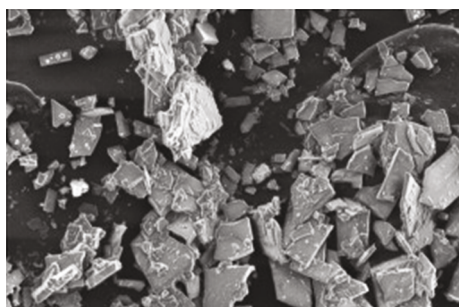


FIGURE 5: SEM analysis of SA-Ag-NP.

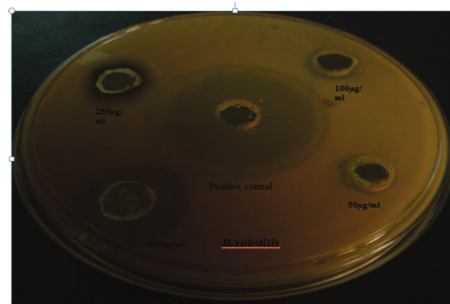


FIGURE 6: Antimicrobial activity of SA-Ag-NP.

**2.1.12. DSC Analysis.** Thermograms of SA-Ag-NP were obtained using a Shimadzu DSC-50. The biomaterial was heated from 20 to 350°C at a constant heating rate of 10 c/min under the nitrogen environment [23].

**2.1.13. TGA.** Thermogravimetric analysis (TGA) was carried out for SA-Ag-NP-incorporated biomaterials. The biomaterial was placed in alumina crucibles heated at varying temperatures in a nitrogen environment [24].

### 3. Result and Discussion

Treating chronic wounds becomes a major concern around the world [25]. The proper healing of chronic wounds depends on the efficacy of the therapeutic agent [26]. The therapeutic agent should prevent all the ailments associated with chronic wounds and should act as temporary skin till the proper closure happens. Apart from the therapeutic material, the drug should be released in a sustained manner. A single therapeutic model cannot achieve the proper

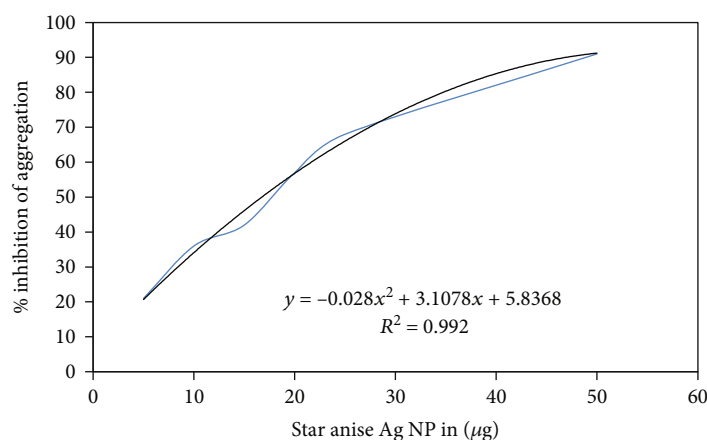


FIGURE 7: Inhibition of aggregation by SA-Ag-NP.

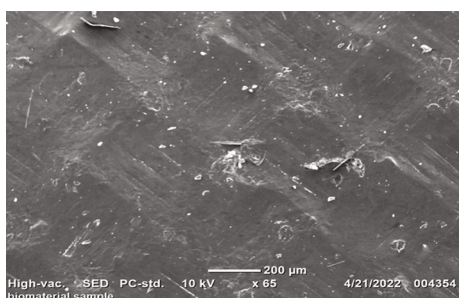


FIGURE 8: SEM analysis of SA-Ag-NP-incorporated chitosan biomaterials.

healing of chronic wounds [27]. Considering here in this study, we prepared Ag-NP using star anise and incorporated it into chitosan biomaterial.

Through GCMS analysis, it was found that star anise extract has more potent compounds; more than 40 compounds were detected in GCMS analysis as shown in Figure 1. From the results, it was inferred that a lot of bioactive phenolic compounds were present in the extract [28]. These bioactive compounds enhance the healing of wounds if applied to the wound environment.

**3.1. Antioxidant Assay.** Herbal plants undoubtedly have more antioxidant potency, especially components derived out of aromatic substances will have more antioxidant potency [29]. Through GCMS analysis, it was inferred that the extract has more phenolic compounds. DPPH assay revealed that the star anise extract efficiently scavenges the radicals. IC50 concentration of the extract was found to be 10 μg/ml. At the concentration of 25 μg/ml, star anise extract was able to scavenge almost all the radicals. Hydroxyl radical assay also depicts the same. Star anise extract shows IC50 of 10 μg/ml for hydroxyl radical as shown in Figure 2.

**3.2. The Characterization of Star Anise Ag-NP by UV-Visible Spectrophotometry.** Figure 3 shows the UV-Vis spectrum of star anise Ag-NP. The metal nanoparticle has shown a characteristic peak at 465 nm. Silver nanoparticles show a peak in the range of 380–480 depending on their physical characteristics such as size, shape, and distribution [30]. The charac-

teristic peak obtained in the range of 465 nm depicts the successful formation of star anise Ag-NP as shown in Figure 4.

**3.3. Morphological Characterization of SA-Ag-NP by SEM.** The Ag-NP was characterized for its size shape and morphology through SEM analysis. From Figure 5, it was inferred that SA-Ag-NP shows a solid crystal-like structure with little agglomeration. The agglomeration of the Ag-NP may be due to the hydroxyl groups present in the star anise extract [31, 32].

**3.4. Antimicrobial Activity of SA-Ag-NP.** Figure 6 depicts the antibacterial activity of synthesized Ag-NP. From the results, it was inferred that Ag-NP at the concentration of 500 μg/ml showed high potent activity on par with third-generation antibiotics. The zone of inhibition for 500 μg/ml Ag-NP was found to be 21 mm.

**3.5. Protein Aggregation or Denaturation Assay.** One of the important factors for unwanted low-grade or high-grade inflammatory responses is due to the denaturation of protein [33]. To ascertain whether denaturation or aggregation of the SA-Ag-NP protein has anti-inflammatory properties. From the assay, it was inferred that SA-Ag-NP can inhibit the denaturation of proteins which indirectly depicts that SA-Ag-NP is a potent anti-inflammatory substance as shown in Figure 7.

**3.6. Characterization of SA-Ag-NP-Incorporated Chitosan Biomaterials.** SA-Ag-NP-incorporated chitosan biomaterial was subjected SEM analysis to study texture, damage of biomaterial while preparation, and microenvironment. The reduced pore size of the biomaterial acts as a good wound dressing as it cannot be damaged while applied to the wounds. From the SEM analysis, it was found that the biomaterials do not have pores, it was flat, and there were gaps in the material. It has uniform morphology throughout its structure, and it can act as perfect temporary skin as shown in Figure 8.

**3.7. FTIR Analysis of SA-Ag-NP-Incorporated Chitosan Biomaterials.** Figure 9 shows the FTIR spectrum of SA-Ag-NP-incorporated chitosan biomaterials. FTIR was generally

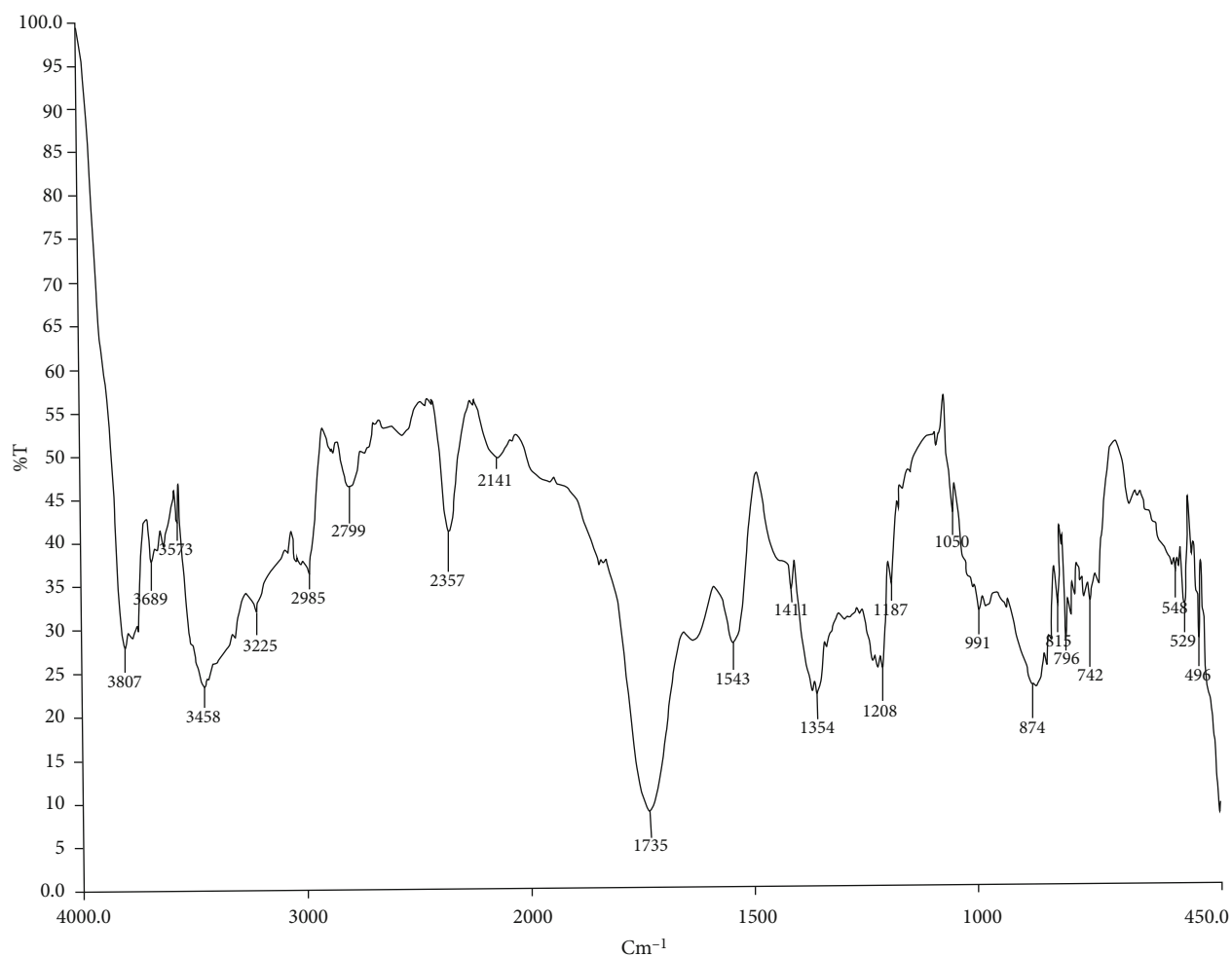


FIGURE 9: FTIR analysis of SA-Ag-NP-incorporated chitosan biomaterials.

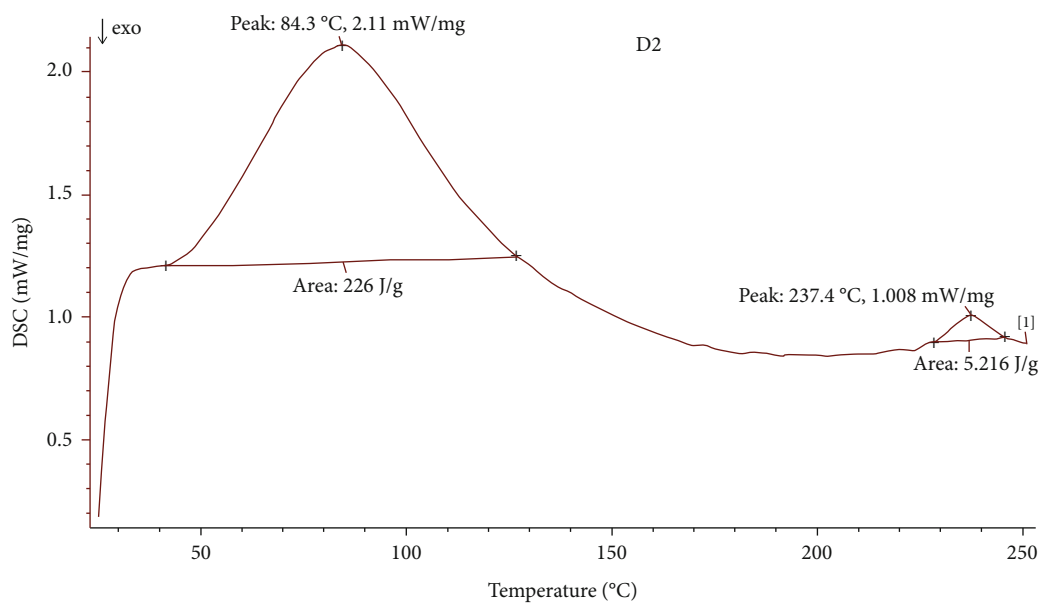


FIGURE 10: Dynamic scanning calorimetry for SA-Ag-NP-incorporated chitosan biomaterials.



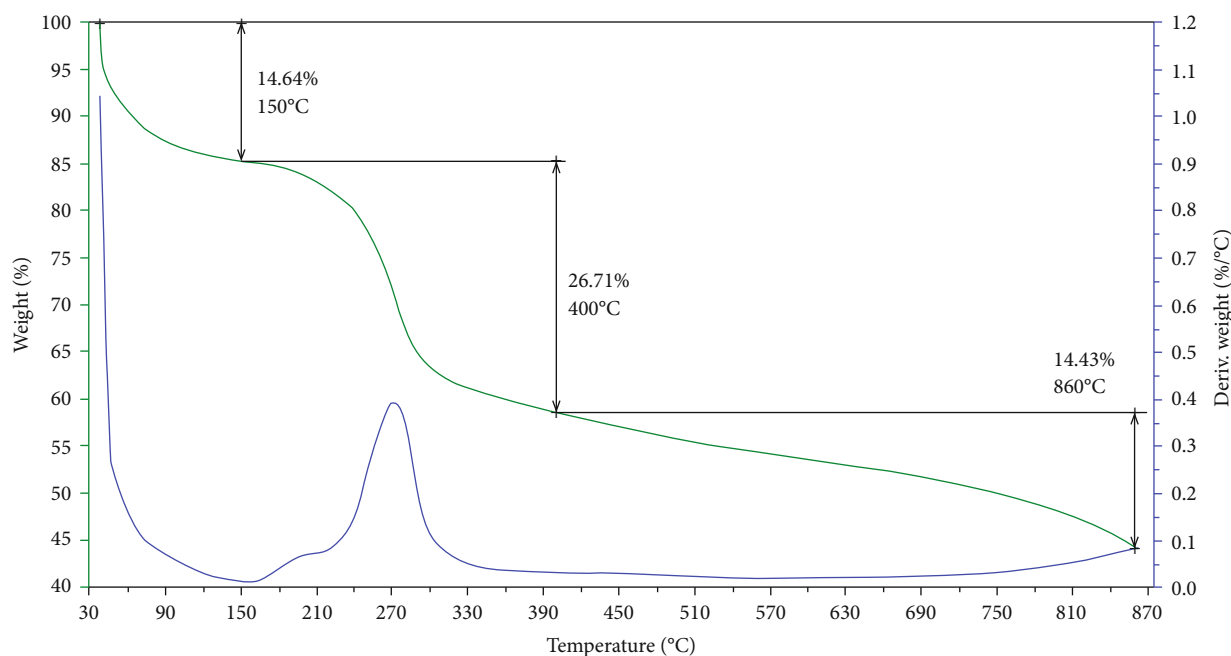


FIGURE 11: Weight vs. temperature for SA-Ag-NP-incorporated chitosan biomaterials.

used to study the functional group. Here in this, we have done FTIR to confirm that SA-Ag-NP was successfully incorporated into the biomaterials. From the results, it was inferred that a lot of peaks were observed. The peaks were noticed at  $3807\text{ cm}^{-1}$ ,  $2985\text{ cm}^{-1}$ ,  $2799\text{ cm}^{-1}$ ,  $2352\text{ cm}^{-1}$ ,  $2141\text{ cm}^{-1}$ ,  $1735\text{ cm}^{-1}$ ,  $1543\text{ cm}^{-1}$ ,  $1411\text{ cm}^{-1}$ , and  $1354\text{ cm}^{-1}$ . The observed OH stretching may be due to the presence of phenols and alcohols. The stretching vibration C-H and C=O suggest the presence of functional aldehydes and other aromatic compounds [28, 34].

**3.8. Dynamic Scanning Calorimetry (DSC) and TGA for SA-Ag-NP-Incorporated Chitosan Biomaterials.** The thermal stability of biomaterials was studied using DSC and TGA. From the DSC results, it was inferred that SA-Ag-NP-incorporated chitosan biomaterials have more thermal stability and can be acted as a good biomaterial [28]. The degradation was observed at  $237^{\circ}\text{C}$ . It was also confirmed with TGA, as shown in Figures 10 and 11.

## 4. Conclusion

The characterization studies reveal that SA-Ag-NP was synthesized efficiently. The characteristic peak at  $465\text{ nm}$  in UV-visible spectroscopy and SEM analysis suggests and confirms the formation of SA-Ag-NP.

- (i) DPPH assay and hydroxyl radical proves that star anise can easily clear off free radicals in the wound environment
- (ii) The SA-Ag-NP is further incorporated into the chitosan polymer

- (iii) This chitosan biomaterial can be utilized as a wound water adsorbent
- (iv) The SA-Ag-NP-incorporated chitosan biomaterials were characterized by various physicochemical analyses; from the analysis, it was inferred that SA-Ag-NP-incorporated chitosan biomaterials can act good biomaterial for chronic wounds

## Data Availability

There are no relevant data to be made available.

## Conflicts of Interest

The authors declare no conflict of interest.

## References

- [1] M. Mostafa, N. G. Kandile, M. K. Mahmoud, and H. M. Ibrahim, "Synthesis and characterization of polystyrene with embedded silver nanoparticle nanofibers to utilize as antibacterial and wound healing biomaterial," *Heliyon*, vol. 8, no. 1, p. e08772, 2022.
- [2] I. Ijaz, A. Bukhari, E. Gilani et al., "Green synthesis of silver nanoparticles using different plants parts and biological organisms, characterization and antibacterial activity," *Environmental Nanotechnology, Monitoring & Management*, vol. 18, p. 100704, 2022.
- [3] M. Abbasi, M. Sohail, M. U. Minhas, J. Iqbal, A. Mahmood, and A. J. Shaikh, "Folic acid-functionalized nanoparticles-laden biomaterials for the improved oral delivery of hydrophobic drug in colorectal cancer," *Journal of Drug Delivery Science and Technology*, vol. 71, article 103287, 2022.

- [4] V. P. Veeraraghavan, N. D. Periadurai, T. Karunakaran, S. Hussain, K. M. Surapaneni, and X. Jiao, "Green synthesis of silver nanoparticles from aqueous extract of *Scutellaria barbata* and coating on the cotton fabric for antimicrobial applications and wound healing activity in fibroblast cells (L929)," *Saudi Journal of Biological Sciences*, vol. 28, no. 7, pp. 3633–3640, 2021.
- [5] F. Sterpione, K. Mas, M. Rippon et al., "The clinical impact of hydroresponsive dressings in dynamic wound healing: part I," *Journal of Wound Care*, vol. 30, no. 1, pp. 15–24, 2021.
- [6] H. M. Li, Q. G. Zhang, N. N. Guo, A. M. Zhu, and Q. L. Liu, "Ultrafine polystyrene nanofibers and its application in nanofibrous membranes," *Chemical Engineering Journal*, vol. 264, pp. 329–335, 2015.
- [7] N. F. Joughi, M. R. Farahpour, M. Mohammadi, S. Jafarirad, and S. Mahmazi, "Investigation on the antibacterial properties and rapid infected wound healing activity of silver/laterite/chitosan nanocomposites," *Journal of Industrial and Engineering Chemistry*, vol. 111, pp. 64–75, 2022.
- [8] S. K. Karuppanan, J. Bushion, R. Ramalingam et al., "Fabrication, characterization and *in vitro* evaluation of *Melia dubia* extract infused nanofibers for wound dressing," *Journal of King Saud University-Science*, vol. 34, no. 4, p. 101931, 2022.
- [9] S. Naraginti, P. L. Kumari, R. K. Das, A. Sivakumar, S. H. Patil, and V. V. Andhalkar, "Amelioration of excision wounds by topical application of green synthesized, formulated silver and gold nanoparticles in albino wistar rats," *Materials Science and Engineering: C*, vol. 62, pp. 293–300, 2016.
- [10] S. R. Kanatt, S. P. Chawla, and A. Sharma, "Antioxidant and radio-protective activities of lemon grass and star anise extracts," *Food Bioscience*, vol. 6, pp. 24–30, 2014.
- [11] S. E. Aly, B. A. Sabry, M. S. Shaheen, and A. S. Hathout, "Assessment of antimycotoxigenic and antioxidant activity of star anise (*Illicium verum*) *in vitro*," *Journal of the Saudi Society of Agricultural Sciences*, vol. 15, no. 1, pp. 20–27, 2016.
- [12] H. Hu, F. Luo, Q. Zhang et al., "Berberine coated biocomposite hemostatic film based alginate as absorbable biomaterial for wound healing," *International Journal of Biological Macromolecules*, vol. 209, no. Part B, pp. 1731–1744, 2022.
- [13] S. Wang, Y. Hou, S. Zhang et al., "Sustained antibacterial activity of berberine hydrochloride loaded supramolecular organo-clay networks with hydrogen-bonding junctions," *Journal of Materials Chemistry B*, vol. 6, no. 30, pp. 4972–4984, 2018.
- [14] M. A. Khan and M. Mujahid, "A review on recent advances in chitosan based composite for hemostatic dressings," *International Journal of Biological Macromolecules*, vol. 124, pp. 138–147, 2019.
- [15] R. Singh, K. Shitiz, and A. Singh, "Chitin and chitosan: biopolymers for wound management," *International wound journal*, vol. 14, no. 6, pp. 1276–1289, 2017.
- [16] F. A. Lubis, N. A. Malek, N. S. Sani, and K. Jemon, "Biogenic synthesis of silver nanoparticles using *Persicaria odorata* leaf extract: Antibacterial, cytocompatibility, and *in vitro* wound healing evaluation," *Particuology*, vol. 70, pp. 10–19, 2022.
- [17] H. L. Loo, B. H. Goh, L. H. Lee, and L. H. Chuah, "Application of chitosan-based nanoparticles in skin wound healing," *Asian Journal of Pharmaceutical Sciences*, vol. 17, no. 3, pp. 299–332, 2022.
- [18] S. Naz, S. Alam, W. Ahmed et al., "Therapeutic potential of selected medicinal plant extracts against multi-drug resistant *Salmonella enterica* serovar Typhi," *Saudi Journal of Biological Sciences*, vol. 29, no. 2, pp. 941–954, 2022.
- [19] B. Halliwell and J. M. C. Gutteridge, *Free radicals in biology and medicine*, vol. 3, Clarendon Press, 1989.
- [20] A. I. Journal, S. M. Mousavi, S. A. Hashemi et al., "Green synthesis of silver nanoparticles toward bio and medical applications : review study," *Artificial cells, nanomedicine, and biotechnology*, vol. 46, pp. S855–S872, 2018.
- [21] J. Singh, N. Kapoor, and A. Verma, "A study to evaluate the effect of phyto-silver nanoparticles synthesized using *Oxalis stricta* plant leaf extract on extracellular fungal amylase and cellulose," *Materials Today: Proceedings*, vol. 18, pp. 1342–1350, 2019.
- [22] K. Järbrink, G. Ni, H. Sönnergren et al., "The humanistic and economic burden of chronic wounds: a protocol for a systematic review," *Systematic reviews*, vol. 6, no. 1, pp. 1–7, 2017.
- [23] B. Sarmiento, D. Ferreira, F. Veiga, and A. Ribeiro, "Characterization of insulin-loaded alginate nanoparticles produced by ionotropic pre-gelation through DSC and FTIR studies," *Carbohydrate Polymers*, vol. 66, no. 1, pp. 1–7, 2006.
- [24] J. M. Rami, C. D. Patel, C. M. Patel, and M. V. Patel, "Thermogravimetric analysis (TGA) of some synthesized metal oxide nanoparticles," *Materials Today: Proceedings*, vol. 43, pp. 655–659, 2021.
- [25] S. Settipalli, *A robust market rich with opportunities: advanced wound dressings*, vol. 360, pp. 229–259, 2015.
- [26] D. J. Kamothi, V. Kant, B. L. Jangir, V. G. Joshi, M. Ahuja, and V. Kumar, "MunishAhuja, Vinod Kumar, Novel preparation of bilirubin-encapsulated pluronic F-127 nanoparticles as a potential biomaterial for wound healing," *European Journal of Pharmacology*, vol. 919, p. 174809, 2022.
- [27] Y. Huang, X. Zhao, Z. Y. Zhang et al., "Degradable gelatin-based IPN cryogel hemostat for rapidly stopping deep non-compressible hemorrhage and simultaneously improving wound healing Chem," *Maternité*, vol. 32, no. 15, pp. 6595–6610, 2020.
- [28] M. Shashikant, A. Bains, P. Chawla et al., "In-vitro antimicrobial and anti-inflammatory activity of modified solvent evaporated ethanolic extract of *Calocybe indica*: GCMS and HPLC characterization," *International Journal of Food Microbiology*, vol. 376, p. 109741, 2022.
- [29] S. Taghavi Fardood and A. Ramazani, "Green synthesis and characterization of copper oxide nanoparticles using coffee powder extract," *Journal of Nanostructures*, vol. 6, pp. 167–171, 2016.
- [30] A. Ahmeda, A. Zangeneh, and M. M. Zangeneh, "Green synthesis and chemical characterization of gold nanoparticle synthesized using *Camellia sinensis* leaf aqueous extract for the treatment of acute myeloid leukemia in comparison to daunorubicin in a leukemic mouse model," *Applied organometallic chemistry*, vol. 34, no. 3, 2020.
- [31] S. Ashraf, A. Z. Abbasi, C. Pfeiffer et al., "Protein-mediated synthesis, pH-induced reversible agglomeration, toxicity and cellular interaction of silver nanoparticles," *Colloids and Surfaces B: Biointerfaces*, vol. 102, pp. 511–518, 2013.
- [32] M. M. Zangeneh, "Green synthesis and formulation a modern chemotherapeutic drug of *Spinacia oleracea* L. leaf aqueous extract conjugated silver nanoparticles; Chemical characterization and analysis of their cytotoxicity, antioxidant, and anti-acute myeloid leukemia properties in comparison to doxorubicin in a leukemic mouse model," *Applied organometallic chemistry*, vol. 34, no. 1, 2020.



- [33] N. Senthilkumar, E. Nandhakumar, P. Priya, D. Soni, M. Vimalan, and I. VethaPotheher, "Synthesis of ZnO nanoparticles using leaf extract of *Tectona grandis* (L.) and their anti-bacterial, anti-arthritic, anti-oxidant and in vitro cytotoxicity activities," *New Journal of Chemistry*, vol. 41, no. 18, pp. 10347–10356, 2017.
- [34] Y. Wang, A. Chinnathambi, O. Nasif, and S. A. Alharbi, "Green synthesis and chemical characterization of a novel anti-human pancreatic cancer supplement by silver nanoparticles containing *Zingiber officinale* leaf aqueous extract," *Arabian Journal of Chemistry*, vol. 14, no. 4, p. 103081, 2021.